

Source characterization of the 20th May 2024 M_D 4.4 Campi Flegrei caldera earthquake through a joint source-propagation probabilistic inversion

M. Supino *, L. Scognamiglio ¹, L. Chiaraluca ¹, C. Doglioni ¹, A. Herrero ¹

¹Istituto Nazionale di Geofisica e Vulcanologia, Roma, Italy

Author contributions: *Conceptualization:* M. Supino. *Formal Analysis:* M. Supino. *Investigation:* M. Supino, L. Scognamiglio, L. Chiaraluca, C. Doglioni, A. Herrero. *Methodology:* M. Supino. *Writing – original draft:* M. Supino. *Writing – review & editing:* M. Supino, L. Scognamiglio, L. Chiaraluca, C. Doglioni, A. Herrero.

Abstract On May 20, 2024, an earthquake of magnitude M_D 4.4 nucleated at shallow depth (2.6 km) in the Campi Flegrei caldera (Southern Italy), a densely populated area where an increase in seismic activity has been observed since 2019 attributable to an on-going unrest episode. While the magnitude was moderate, the event produced a strong ground shaking with an observed maximum peak ground acceleration of 3.58 m s^{-2} , and several buildings were damaged. Here, we characterize the earthquake source using a probabilistic joint source-propagation spectral inversion in the Fourier space. We estimate a moment magnitude $M_w = 3.70 \pm 0.13$ and a corner frequency $f_c = 1.11 \pm 0.19 \text{ Hz}$. Assuming a circular rupture model, we estimate a source radius $r = 400 \pm 70 \text{ m}$ and a stress drop $\Delta\sigma = 3.2 \pm 2.2 \text{ MPa}$. The estimated stress drop suggests that future earthquakes in the hypocentral region, considering a possible rupture length of 3 km suggested by previous studies, can have magnitude increased by 1.2 ± 0.3 units with respect to May 20th event. A systematic source characterization of the recent seismicity in the caldera would help in estimating the expected ground motion from future large-magnitude events.

Production Editor:
Kiran Kumar Thingbaijam
Tiegan Hobbs
Handling Editor:
Kiran Kumar Thingbaijam
Copy & Layout Editor:
Hannah F. Mark

Received:
June 26, 2024
Accepted:
July 29, 2024
Published:
August 5, 2024

1 Introduction

The Campi Flegrei caldera is a volcanic structure located close to Naples (Southern Italy), in a densely populated area inhabited by almost two million people. In recent years, two unrest episodes associated with ground uplift occurred in the caldera (from 1969 to 1972 and from 1982 to 1984). The uplift of the caldera resumed in 2005, and since 2019 an increase in seismic activity has been observed (e.g., I.N.G.V.-O.V., 2024).

Historically, duration magnitude M_D has been a common magnitude measurement among several seismic networks recording microearthquakes (Lee and Stewart, 1981). Osservatorio Vesuviano (OV) is the section of the National Institute of Geophysics and Volcanology (INGV) in charge of the geophysical monitoring of the Campi Flegrei caldera. OV is currently using M_D as routine magnitude measurement for the earthquakes occurring in the region (Orsi et al., 1999; Petrosino et al., 2008). The M_D 4.4 event, occurred on May, 20th, was the strongest event recorded in the region during the last 40 years, and limited knowledge exists about the scaling of M_D with parameters directly related to the physics of the source, such as the seismic moment M_0 , when the size of the earthquake is large as the M_D 4.4 event.

The earthquake produced a strong ground shaking. While the event magnitude was moderate, the maximum peak ground acceleration (PGA) observed among

all the available seismic stations was 3.58 m s^{-2} . For instance, this is equal to 55.6% of the maximum PGA observed after the M_w 6.1 L'Aquila earthquake occurred on April 6th, 2009. Clearly, the shallow depth of the earthquake (2.6 km) contributes to determining the shaking and the significant seismic hazard posed by such relatively small events. Overall, the seismic risk assessment in the area must also take into account the high vulnerability and the peculiar exposure factor, with ~15,500 residential buildings and ~85,000 people living in the higher risk zone identified by the Italian Government in October 2023 (Decreto-legge 140/2023).

In this work, we use the probabilistic approach proposed by Supino et al. (2019) to characterize the source of the M_D 4.4 earthquake by inverting displacement amplitude spectra. We estimate the joint a-posteriori probability density function of source parameters seismic moment M_0 , corner frequency f_c , high-frequency decay γ and of propagation parameter Q' , which models the anelastic attenuation of seismic waves. From M_0 we obtain the moment magnitude M_w (Hanks and Kanamori, 1979), while assuming a circular rupture model f_c is used to estimate the source radius r . Finally, both M_0 and r are used to estimate the earthquake stress drop $\Delta\sigma$.

*Corresponding author: mariano.supino@ingv.it

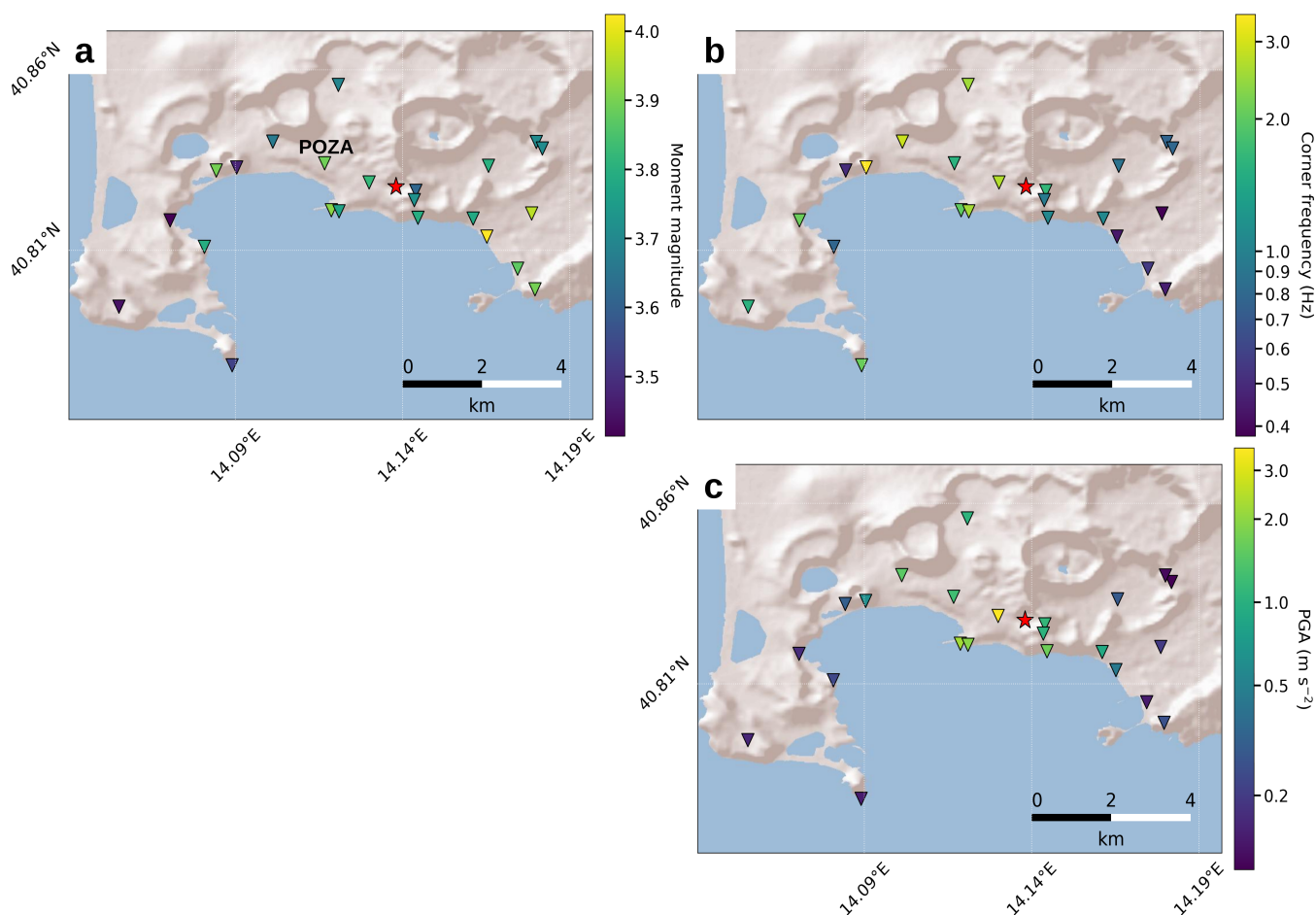


Figure 1 Map with event, stations, estimated parameters and observed PGA. **a.** The earthquake epicenter is shown (red star) together with the stations (colored triangles) used for earthquake source characterization. The color of station markers is according to the moment magnitude. **b.** As in a, with color according to corner frequency **c.** As in a, with color according to observed PGA. Color bar in panels (b) and (c) has a log scale. The hypocentral distance of the stations ranges from 2.88 to 8.35 km.

2 Data and Method

We analyze the earthquake that occurred in the Campi Flegrei caldera (Italy) on May 20th, 2024 at 18:10:03 (UTC Time) (red star in Figure 1). For the analysis, we adopt the hypocenter location estimated by INGVOV. The events in the region are routinely located using a 1D-velocity model (Orsi et al., 2004; Tramelli et al., 2021). It is noted that the uncertainty in the hypocenter location and velocity model will impact the estimation of moment magnitude (see Eq. 1 and Supplementary Text S1). We invert data from 23 seismic stations (Figure 1) from the seismic monitoring network deployed by INGVOV, and the Accelerometric National Network (RAN) deployed by the Department of Italian Civil Protection (DPC). All data are publicly available through web services or web pages (see Data Availability section). We use acceleration records for all the stations, except for one station CSMN for which only velocity records were available.

We invert S-wave displacement amplitude spectra using the probabilistic method by Supino et al. (2019). The method has been used to characterize the earthquake source in different tectonic settings and with different type of seismic data (Strumia et al., 2024; Supino

et al., 2019, 2020), and is part of the SCEC/USGS Community Stress Drop Validation Study (Baltay et al., 2024). The forward operator along with the pre-processing and processing parameters used for the analysis closely follow Supino et al. (2019), and are also described in the Supplementary material (Text S1).

We estimate for each station the joint source-propagation a-posteriori probability density function (PDF) $\sigma(\mathbf{m} = \log M_0, f_c, \gamma, Q')$ (Figure 2). M_0 (seismic moment), f_c (corner frequency) and γ (high-frequency decay) are the source parameters of a generalized Brune (1970) spectral model, while Q' accounts for both anelastic attenuation quality factor Q and site-dependent attenuation term k_0 . We do not consider a site amplification term in the forward operator, since the inversion is performed on a single event while a set of events is needed to constrain site amplifications. Since average estimates of the source parameters are obtained using data from a large number of stations, we expect that possible site amplification effects are somewhat mitigated.

For each parameter, the single-station solution and uncertainty are the mean and the standard deviation of the corresponding marginal PDF, respectively. The final event solution is the weighted average of single-station

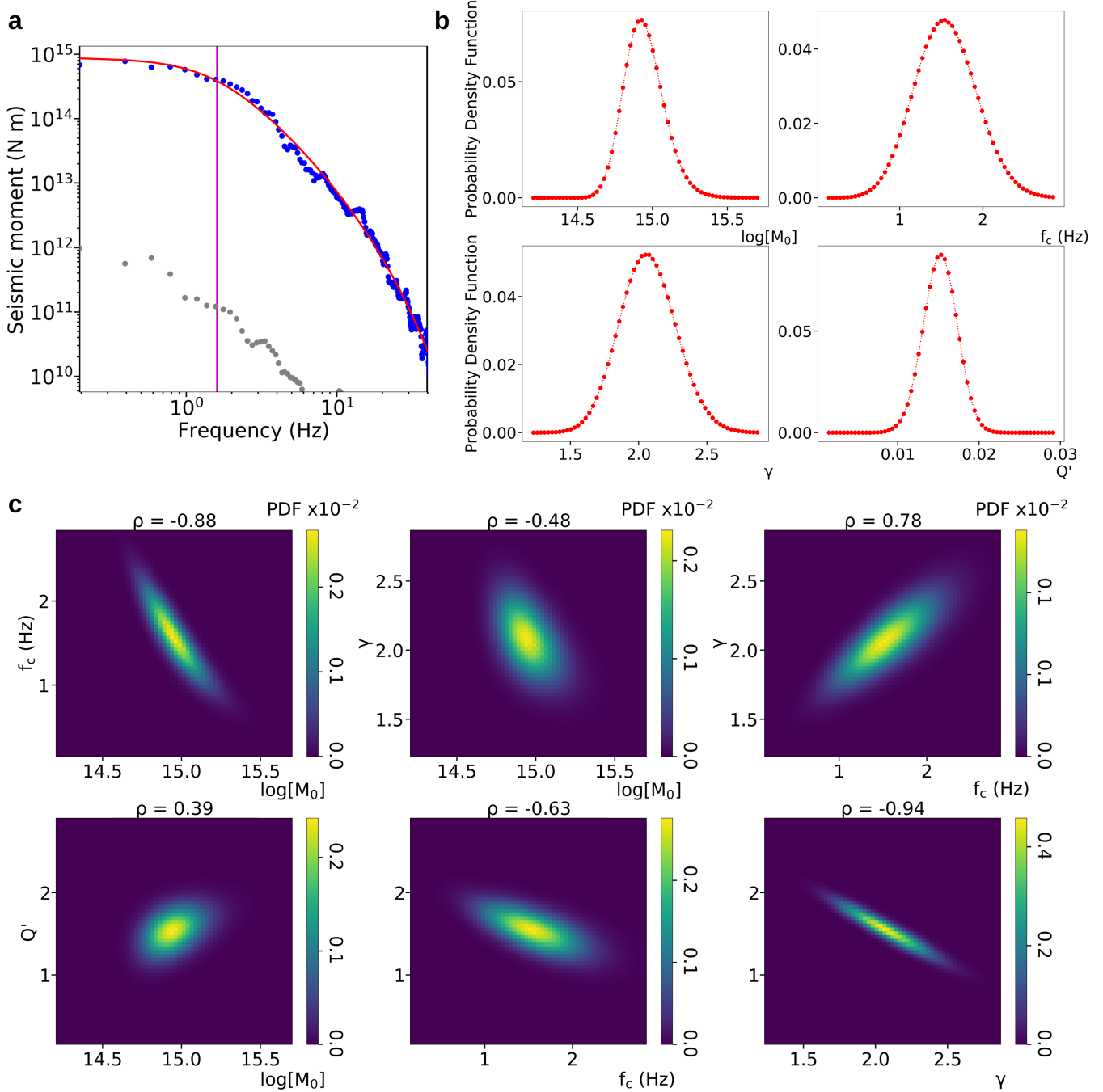


Figure 2 Source and propagation parameter solutions for single-station observation. **a.** S-wave displacement amplitude spectrum (blue dots) in seismic moment units, best fit spectrum (red curve) and noise spectrum (gray dots). The magenta vertical line shows the estimated corner frequency. The noise spectrum is estimated from a signal time window starting from the origin time, with the same length as the inverted S-wave. **b.** 1D marginal PDFs of source parameters $\log M_0$, f_c , γ and propagation parameter Q' . **c.** 2d marginal PDFs for each pair of explored parameters. The correlation coefficient ρ is shown at the top of each heatmap. The analysis shown here is at the station POZA (Figure 1a).

solutions, where the weight is the inverse of the variance estimated from the corresponding marginal PDF.

The methodology that we use in this work to characterize the earthquake source benefits from a probabilistic inversion that provides a PDF as the solution of the spectral inversion, instead of a more common scalar solution. This approach allows to account for between-parameter correlations in both parameter solutions and related uncertainty (Abercrombie, 2021; Supino et al., 2019; Trugman, 2022).

3 Results

Our analysis is characterized by a high spatial resolution thanks to 23 seismic stations located at a hypocentral distance of less than 9 km. This produced a dataset for the event source parameters (Table 1) that is rarely obtained for earthquakes of similar magnitude at such short distances. In addition, the S-wave records are characterized by a very good signal-to-noise ratio (SNR), with $SNR > 3$ in the entire inverted frequency band.

Single-station solutions are well constrained, and

Station	M_w	std(M_w)	f_c (Hz)	std(f_c)	γ	std(γ)	Q'	std(Q')	Q	std(Q)	h_d (km)
BAIP	3.41	0.11	2.1	0.6	2.2	0.3	0.0077	0.0012	130	20	6.349
BAN	4.0	0.2	0.44	0.2	1.56	0.16	0.015	0.0016	67	7	3.829
CBAC	3.79	0.15	0.8	0.3	1.97	0.18	0.0056	0.0012	180	40	5.825
CFMN	3.47	0.07	3.5	0.5	3.1	0.3	0.0036	0.0017	280	130	4.869
CMIS	3.53	0.09	2.1	0.4	2.9	0.3	0.0079	0.0012	126	19	7.401
CMSN	3.71	0.14	0.8	0.2	2.21	0.18	0.0093	0.0015	107	17	4.678
COLB	3.79	0.11	1.1	0.2	2.2	0.11	0.0025	0.0013	400	200	2.879
CPOZ	3.92	0.08	2	0.3	3.1	0.2	0.0091	0.0025	110	30	3.155
CSOB	3.62	0.09	1.6	0.4	2.1	0.2	0.0083	0.0021	120	30	2.871
MPCD	3.44	0.12	1.6	0.5	2.1	0.3	0.0027	0.00095	370	130	8.348
NAAG	3.8	0.16	0.9	0.3	1.9	0.2	0.019	0.0024	54	7	3.577
NABA	3.78	0.16	1.1	0.4	1.9	0.3	0.0091	0.0025	110	30	3.450
NACO	3.87	0.18	0.6	0.2	1.84	0.17	0.012	0.0014	84	10	4.756
NAFG	4.0	0.2	0.38	0.18	1.66	0.16	0.011	0.0014	95	13	4.460
NAP	3.9	0.2	0.5	0.2	1.57	0.18	0.0071	0.001	140	20	5.493
NAPI	3.71	0.15	0.8	0.2	2.33	0.2	0.0067	0.0013	150	30	4.672
POZA	3.89	0.09	1.6	0.4	2.1	0.2	0.015	0.0021	66	9	3.299
POZB	3.66	0.06	2.9	0.4	2.7	0.3	0.011	0.0019	95	17	4.323
POZL	3.9	0.2	0.5	0.3	1.25	0.16	0.015	0.0011	66	5	5.266
POZM	3.72	0.14	0.9	0.4	1.52	0.18	0.019	0.0021	53	6	2.821
POZS	3.82	0.08	2.7	0.6	2.2	0.3	0.019	0.0031	54	9	2.779
POZT	3.77	0.06	2.6	0.2	3.8	0.2	0.0071	0.002	140	40	3.096
POZU	3.69	0.07	2.5	0.4	2.5	0.3	0.0091	0.0017	110	20	4.360

Table 1 Moment magnitude (M_w), corner frequency (f_c), high-frequency decay exponent (γ) and Q' parameter estimated for each station. std() columns indicate the standard deviation of the specified parameter. Q values and errors are obtained from corresponding Q' values and errors, assuming $k_0 = 0$ (see Text S1 and equation S2). h_d column indicates the hypocentral distance of the corresponding station.

show as expected (e.g., Supino et al., 2019) that the largest correlation (correlation coefficient $\rho \sim -0.9$) exists between the parameters $\log M_0 - f_c$ and $\gamma - Q'$, while the smallest ($\rho \sim 0.4$) is between $\log M_0$ and Q' (as shown in Figure 2c).

The collection of single-station spectra shows a remarkable coherency of the low-frequency plateaux (i.e., seismic moments) (Figure 3). Corner frequencies exhibit a larger variability (vertical bars in Figure 3), as usually observed (e.g., Baltay et al., 2024). The asymmetric spatial distribution of f_c values (Figure 1b) – with on average smaller values to the East of the epicenter and larger values to the West – is well correlated with the observed variability of peak ground acceleration (PGA) values (Figure 1c). For stations at a similar epicentral distance, PGAs are smaller in the East direction and larger in the West direction.

We estimate as event source parameter solution $M_w = 3.70 \pm 0.04$ ($M_0 = 4.52 \cdot 10^{14}$ N m), $f_c = 1.11 \pm 0.19$, $\gamma = 2.07 \pm 0.13$; the reported uncertainty is the standard error. The Q' solutions correspond to an average quality factor for the explored propagation medium $Q = 70 \pm 20$, if k_0 is approximated to 0 (Supplementary Text S1). Spectral inversions using P-waves and two different time window lengths show M_w results consistent with S-wave inversion, although probably the proximity of the stations to the source does not allow properly isolation of the P-phase in the observed signals (Supplementary Text S2, Figure S1).

We point out that the M_w value depends on the modeling assumptions as described in the following equation (also, Supplementary Text S1):

$$M_0 = \Omega_0 \cdot \frac{4\pi \cdot \rho \cdot v_S^3 \cdot r_H}{R_{\theta\varphi} \cdot F_S} \quad (1)$$

Among the parameters, S-wave velocity (v_S), being exposed to the cube, is the most sensitive parameter. We used $v_S^* = 1685$ m s⁻¹, that is the S-wave velocity value of the depth layer corresponding to the hypocenter of the event in the 1D-velocity model used to locate the earthquake. A different possible choice is represented by the average of S-wave velocity values across the depth layers of the velocity model from the hypocenter to the free surface, $\overline{v_S} = 1437$ m s⁻¹ (~15% change from v_S^*). The corresponding moment magnitude would be $M_w = 3.57 \pm 0.04$ while $f_c = 1.11 \pm 0.19$. We note that a similar percentage change in the other parameters would produce a variation in M_w of less than 0.05 units.

For each parameter, we evaluate the epistemic uncertainty – due to input variable uncertainty – as the difference between the two estimates corresponding to the two values considered for v_S , 1685 and 1437 m s⁻¹. We thus define as final uncertainty the largest value between the epistemic uncertainty and the aleatoric uncertainty represented by the standard error: $M_w = 3.70 \pm 0.13$, $f_c = 1.11 \pm 0.19$, $\gamma = 2.07 \pm 0.13$. The estimated M_w is different from the $M_D = 4.4 \pm 0.3$ reported for this event by INGV-OV. Further analysis including a larger

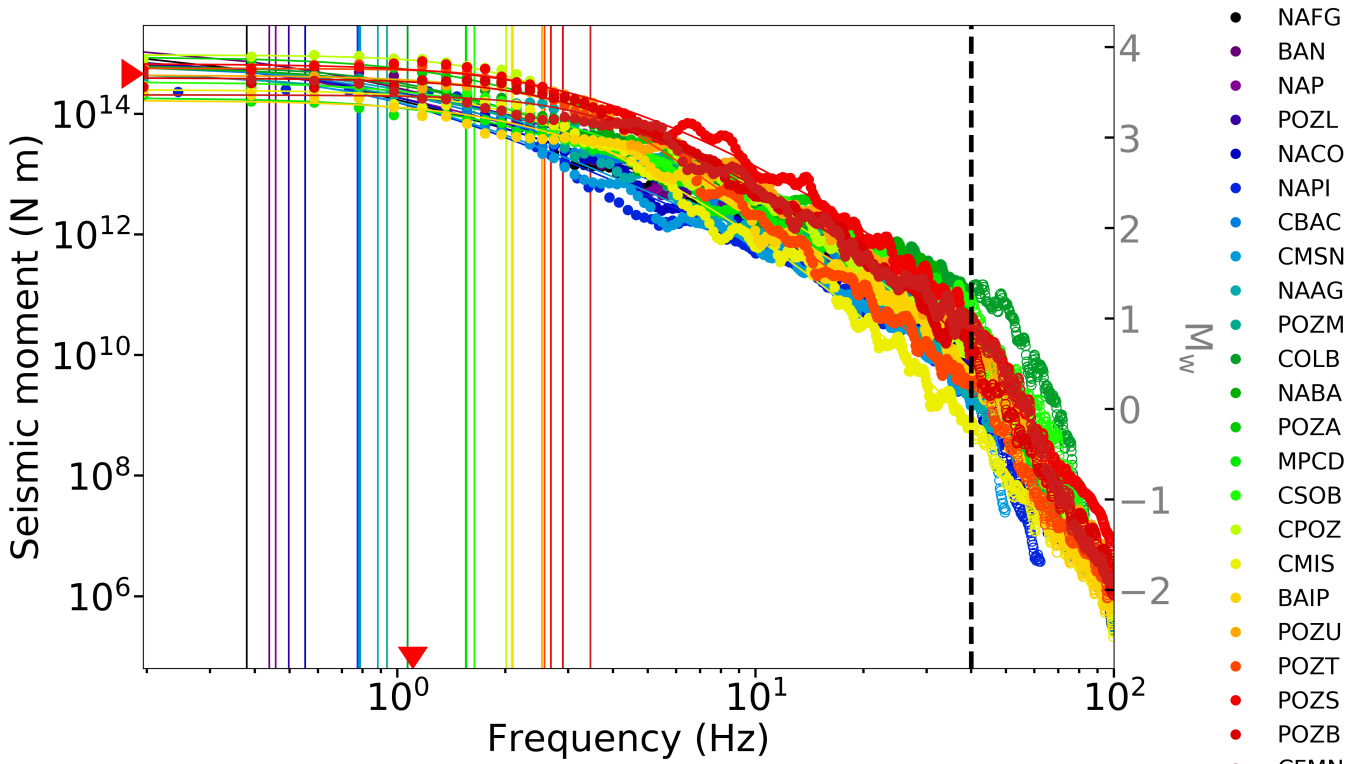


Figure 3 Single-station spectra and final event solution. Single-station displacement spectra (discrete curves), corresponding best-fit solutions (continuous curves) and corner frequency estimates (vertical bars). The red arrows show the final event solution for seismic moment and corner frequency. The black dashed vertical line shows the maximum frequency used for spectral inversions. Colors used to plot the spectra and vertical bars are according to the inverted stations. The listed stations (in the legend) are sorted in ascending order according to estimated corner frequency values.

set of events will help to understand if a systematic shift – or a scaling – between the two magnitude scales exists (e.g., [Drouet et al., 2011](#); [Holt et al., 2021](#)), and to assess the potential impact of such a difference in the statistical analysis of the earthquake catalog (e.g., [Werner and Sornette, 2008](#)).

4 Discussion

The present study demonstrates the feasibility of systematic source characterizations of the earthquakes that occurred in the Campi Flegrei caldera, and supports near future studies on that line. Such studies including a set of events will also help to obtain more precise estimates of source parameters accounting for site amplifications. To the best of our knowledge, volcanic observatories do not routinely estimate moment magnitudes. A possible challenge concerns earthquakes of small magnitude (e.g., $M < 2$), since in that case both the signal-to-noise ratio and the number of available stations with a clear S-wave arrival are expected to decrease.

The source characterization presented in this work can also provide constraints on the potential increase in magnitude in the hypocentral region (Solfatara crater). For the earthquake, we estimate a source radius

$$r = \frac{k \cdot v_S}{f_c} = 400 \pm 70 \text{ m} \quad (2)$$

(e.g., [Hanks and Wyss, 1972](#)), where $f_c = 1.11 \pm 0.19$ Hz is the corner frequency we estimated in this study, and $k = 0.26$ has been obtained by [Kaneko and Shearer \(2014\)](#) assuming a circular rupture model with a rupture velocity $v_R = 0.9 v_S$. Then, we estimate a stress drop

$$\Delta\sigma = \frac{7}{16} \cdot \frac{M_0}{r^3} = 3.2 \pm 2.2 \text{ MPa} \quad (3)$$

([Eshelby, 1957](#)). This stress drop value is in between the two values that can be obtained assuming the [Brune \(1970\)](#) model ($\Delta\sigma = 1.1 \pm 0.8$ MPa, $k = 0.37$) or the [Madariaga \(1976\)](#) model ($\Delta\sigma = 6.1 \pm 4.2$ MPa, $k = 0.21$), that are commonly considered in literature as the two end-members for possible values that k , and therefore r and $\Delta\sigma$, could assume (e.g., [Kaneko and Shearer, 2014](#), also see Figure S2).

Recently, [Danesi et al. \(2024\)](#) relocated the events (since 2005) in the study area, and showed that a ~ 3 km long structure could exist below the Solfatara crater. The depth of which is comparable with that of the event investigated in the present study. If we consider a 3 km length based on [Danesi et al. \(2024\)](#) as the maximum possible rupture dimension (1.5 km as the source radius for a circular rupture), then the estimated magnitude corresponds to $M_w = 4.9 \pm 0.3$ assuming the stress drop $\Delta\sigma = 3.2 \pm 2.2$ MPa obtained in the present study. This suggests that, in case the structure undergoing a future rupture is the one highlighted by [Danesi et al. \(2024\)](#), it is not possible to exclude an increase in magnitude of

$\Delta M_w = 1.2 \pm 0.3$ units compared to the main event that occurred on May, 20th 2024. The possible increase in magnitude slightly changes to $\Delta M_w = 1.3 \pm 0.3$ if $v_S = 1437 \text{ m s}^{-1}$ is assumed.

The scenario presented here raises a challenging question about the expected maximum PGA if such an increase in magnitude will occur. Concerning the observed ground shaking levels (Figure 1), we highlight the following: (1) the stations at a similar epicentral distance (but in different directions, i.e., west and east from the epicenter) have different PGA (Figure 1c); and (2) the spatial distribution of the estimated corner frequencies (Figure 1b) is remarkably consistent with the observed PGAs. Considering previous work relative to ground motion prediction equations in Italy (e.g., Bindi et al., 2009, 2011), these observations suggest the need to account for source-directivity in the ground motion modeling of the Campi Flegrei caldera, even for moderate magnitude events (e.g., Colavitti et al., 2022; Jayaram and Baker, 2010; Pacor et al., 2016). Alternatively, the coherence between f_c and PGA could be due to site amplification effects, although this would require frequency-dependent amplifications that coherently shift the corner frequencies (without producing in the observed spectra clear amplitude peaks or deviations from the Brune-type shape). In any case, rigorous and systematic source characterization is warranted for the recent events in the Campi Flegrei caldera, which in turn will enable better characterization of future large events in the region, and support ground motion modeling of those events. An assessment of the expected response of the buildings to such ground motion should follow.

Acknowledgements

We thank the Editor, Dr. Kiran Kumar Thingbaijam, and an anonymous Reviewer for their careful reviews which helped improve the manuscript.

5 Data and code availability

The parameters estimated in this study are provided in Table 1. The INGV event-ID and location-ID of the event (investigated in the present study) are 38759141 and 127958121, respectively. The INGV catalog information can be found online at <https://terremoti.ingv.it/event/38759141> (last accessed, July 2024). The seismological time series used for this analysis are available from EIDA (<https://eida.ingv.it>, last accessed July 2024) and DPC-RAN (<https://ran.protezionecivile.it>, last accessed July 2024).

6 Competing interests

There are no competing interests.

References

- Abercrombie, R. E. Resolution and uncertainties in estimates of earthquake stress drop and energy release. *Philosophical Transactions of the Royal Society A: Mathematical, Physical and Engineering Sciences*, 379(2196):20200131, Mar. 2021. doi: 10.1098/rsta.2020.0131.
- Baltay, A., Abercrombie, R., Chu, S., and Taira, T. The SCEC/USGS Community Stress Drop Validation Study Using the 2019 Ridgecrest Earthquake Sequence. *Seismica*, 3(1), May 2024. doi: 10.26443/seismica.v3i1.1009.
- Bindi, D., Luzi, L., Massa, M., and Pacor, F. Horizontal and vertical ground motion prediction equations derived from the Italian Accelerometric Archive (ITACA). *Bulletin of Earthquake Engineering*, 8(5):1209–1230, June 2009. doi: 10.1007/s10518-009-9130-9.
- Bindi, D., Pacor, F., Luzi, L., Puglia, R., Massa, M., Ameri, G., and Paolucci, R. Ground motion prediction equations derived from the Italian strong motion database. *Bulletin of Earthquake Engineering*, 9(6):1899–1920, Sept. 2011. doi: 10.1007/s10518-011-9313-z.
- Brune, J. N. Tectonic stress and the spectra of seismic shear waves from earthquakes. *Journal of Geophysical Research*, 75(26): 4997–5009, Sept. 1970. doi: 10.1029/jb075i026p04997.
- Colavitti, L., Lanzano, G., Sgobba, S., Pacor, F., and Gallovič, F. Empirical Evidence of Frequency-Dependent Directivity Effects From Small-To-Moderate Normal Fault Earthquakes in Central Italy. *Journal of Geophysical Research: Solid Earth*, 127(6), June 2022. doi: 10.1029/2021jb023498.
- Danesi, S., Pino, N. A., Carlino, S., and Kilburn, C. R. Evolution in unrest processes at Campi Flegrei caldera as inferred from local seismicity. *Earth and Planetary Science Letters*, 626:118530, Jan. 2024. doi: 10.1016/j.epsl.2023.118530.
- Drouet, S., Bouin, M.-P., and Cotton, F. New moment magnitude scale, evidence of stress drop magnitude scaling and stochastic ground motion model for the French West Indies. *Geophysical Journal International*, 187(3):1625–1644, Oct. 2011. doi: 10.1111/j.1365-246x.2011.05219.x.
- Eshelby, J. The determination of the elastic field of an ellipsoidal inclusion, and related problems. *Proceedings of the Royal Society of London Series A. Mathematical and Physical Sciences*, 241 (1226), 1957.
- Hanks, T. C. and Kanamori, H. A moment magnitude scale. *Journal of Geophysical Research: Solid Earth*, 84(B5):2348–2350, May 1979. doi: 10.1029/jb084ib05p02348.
- Hanks, T. C. and Wyss, M. The use of body-wave spectra in the determination of seismic-source parameters. *Bulletin of the Seismological Society of America*, 62(2):561–589, Apr. 1972. doi: 10.1785/bssa0620020561.
- Holt, J., Whidden, K. M., Koper, K. D., Pankow, K. L., Mayeda, K., Pechmann, J. C., Edwards, B., Gök, R., and Walter, W. R. Toward Robust and Routine Determination of Mw for Small Earthquakes: Application to the 2020 Mw 5.7 Magna, Utah, Seismic Sequence. *Seismological Research Letters*, 92(2A):725–740, Jan. 2021. doi: 10.1785/0220200320.
- I.N.G.V.-O.V. Istituto Nazionale di Geofisica e Vulcanologia, Osservatorio Vesuviano May 2024 report, 2024. <https://www.ov.ingv.it/index.php/monitoraggio-e-infrastrutture/bollettini-tutti/bollett-mensili-cf/anno-2024-3/1640-bollettino-mensile-campi-flegrei-2024-05/file>. Accessed: 2024-07-26.
- Jayaram, N. and Baker, J. W. Considering Spatial Correlation in Mixed-Effects Regression and the Impact on Ground-Motion Models. *Bulletin of the Seismological Society of America*, 100(6): 3295–3303, Dec. 2010. doi: 10.1785/0120090366.
- Kaneko, Y. and Shearer, P. M. Seismic source spectra and estimated stress drop derived from cohesive-zone models of circular subshear rupture. *Geophysical Journal International*, 197(2): 1002–1015, Mar. 2014. doi: 10.1093/gji/ggu030.

- Lee, W. and Stewart, S. *Principles and applications of microearthquake networks*, volume 2. Academic press, 1981.
- Madariaga, R. Dynamics of an expanding circular fault. *Bulletin of the Seismological Society of America*, 66(3):639–666, June 1976. doi: 10.1785/bssa0660030639.
- Orsi, G., Civetta, L., Del Gaudio, C., de Vita, S., Di Vito, M., Isaia, R., Petrazzuoli, S., Ricciardi, G., and Ricco, C. Short-term ground deformations and seismicity in the resurgent Campi Flegrei caldera (Italy): an example of active block-resurgence in a densely populated area. *Journal of Volcanology and Geothermal Research*, 91(2–4):415–451, Aug. 1999. doi: 10.1016/s0377-0273(99)00050-5.
- Orsi, G., Di Vito, M. A., and Isaia, R. Volcanic hazard assessment at the restless Campi Flegrei caldera. *Bulletin of Volcanology*, 66(6):514–530, Apr. 2004. doi: 10.1007/s00445-003-0336-4.
- Pacor, F., Gallovič, F., Puglia, R., Luzi, L., and D’Amico, M. Diminishing high-frequency directivity due to a source effect: Empirical evidence from small earthquakes in the Abruzzo region, Italy. *Geophysical Research Letters*, 43(10):5000–5008, May 2016. doi: 10.1002/2016gl068546.
- Petrosino, S., De Siena, L., and Del Pezzo, E. Recalibration of the Magnitude Scales at Campi Flegrei, Italy, on the Basis of Measured Path and Site and Transfer Functions. *Bulletin of the Seismological Society of America*, 98(4):1964–1974, Aug. 2008. doi: 10.1785/0120070131.
- Strumia, C., Trabattoni, A., Supino, M., Baillet, M., Rivet, D., and Festa, G. Sensing Optical Fibers for Earthquake Source Characterization Using Raw DAS Records. *Journal of Geophysical Research: Solid Earth*, 129(1), Jan. 2024. doi: 10.1029/2023jb027860.
- Supino, M., Festa, G., and Zollo, A. A probabilistic method for the estimation of earthquake source parameters from spectral inversion: application to the 2016–2017 Central Italy seismic sequence. *Geophysical Journal International*, 218(2):988–1007, May 2019. doi: 10.1093/gji/ggz206.
- Supino, M., Poiata, N., Festa, G., Vilotte, J. P., Satriano, C., and Obara, K. Self-similarity of low-frequency earthquakes. *Scientific Reports*, 10(1), Apr. 2020. doi: 10.1038/s41598-020-63584-6.
- Tramelli, A., Godano, C., Ricciolino, P., Giudicepietro, F., Caliro, S., Orazi, M., De Martino, P., and Chiodini, G. Statistics of seismicity to investigate the Campi Flegrei caldera unrest. *Scientific Reports*, 11(1), Mar. 2021. doi: 10.1038/s41598-021-86506-6.
- Trugman, D. T. Resolving Differences in the Rupture Properties of M5 Earthquakes in California Using Bayesian Source Spectral Analysis. *Journal of Geophysical Research: Solid Earth*, 127(4), Apr. 2022. doi: 10.1029/2021jb023526.
- Werner, M. J. and Sornette, D. Magnitude uncertainties impact seismic rate estimates, forecasts, and predictability experiments. *Journal of Geophysical Research: Solid Earth*, 113(B8), Aug. 2008. doi: 10.1029/2007jb005427.

The article *Source characterization of the 20th May 2024 M_D 4.4 Campi Flegrei caldera earthquake through a joint source-propagation probabilistic inversion* © 2024 by M. Supino is licensed under CC BY 4.0.